International Journal of Architectural, Civil and Construction Sciences
ISSN: 2415-1734
Vol:9, No:3, 2015

Seismic Behavior of Steel Moment-Resisting Frames for Uplift Permitted in Near-Fault Regions

M. Tehranizadeh, E. Shoushtari Rezvani

***Abstract*—**Seismic performance of steel moment-resisting frame structures is investigated considering nonlinear soil-structure interaction (SSI) effects. 10-, 15-, and 20-story planar building frames with aspect ratio of 3 are designed in accordance with current building codes. Inelastic seismic demands of the superstructure are considered using concentrated plasticity model. The raft foundation system is designed for different soil types. Beam-on-nonlinear Winkler foundation (BNWF) is used to represent dynamic impedance of the underlying soil. Two sets of pulse-like as well as no-pulse near-fault earthquakes are used as input ground motions. The results show that the reduction in drift demands due to nonlinear SSI is characterized by a more uniform distribution pattern along the height when compared to the fixed-base and linear SSI condition. It is also concluded that beneficial effects of nonlinear SSI on displacement demands is more significant in case of pulse-like ground motions and performance level of the steel moment-resisting frames can be enhanced.

***Keywords*—**Soil-structure interaction, uplifting, soil plasticity, near-fault earthquake, tall building.

I. INTRODUCTION

NEAR-FAULT ground motions usually contain a few long-period large-amplitude pulses. These pulse-type motions are generally particular to the forward direction, where the fault rupture propagates toward the site at a velocity close to shear wave velocity [1]. Due to the specific pattern of shear deformations, these pulses are observed in the direction perpendicular to the fault (i.e. fault-normal component) [2]. In addition to forward directivity long-period pulses, near-fault earthquake records entail high-frequency contents and also may contain permanent displacement, so-called fling-step [3]. Among mentioned characteristics, i.e. directivity pulses, high-frequency content and fling-step, the first one has attracted more attention as a critical issue in the design of structures in the near-fault regions.

After 1994 Northridge and 1995 Kobe earthquakes, and consequent damage and decimation in urban areas whose structures were designed based on modern seismic codes, the deficiencies of modern codes of practice in near-fault seismic design were revealed. In response to this need, much effort has been devoted to study the seismic performance of elastic and inelastic single- and multi-dof systems subjected to these types of excitations [4]-[6].

The vast majority of studies on seismic structural performance subjected to near-fault earthquakes are commonly performed under the assumption that the structural elements are fixed at their base against translation, settlement, and rotation. In fact, structures excited by earthquake ground shaking develop inertial forces, which in turn introduce base shear, moment, and axial forces to the foundation system. Unless the foundation system and supporting soil are rigid, those demands will introduce foundation displacements and rotations. Although not widely used in practice, engineering guidelines exist for simple evaluation of soil-structure interaction (SSI) effects. First generation of such guidelines is intended for use with force-based characterization of seismic design, as is commonly used for new building construction. These procedures were introduced by ATC [7] and an updated version is currently published in the NEHRP Recommended Provisions for Seismic Regulations for New Buildings and Other Structures FEMA-450 [8].

Based on more recent findings, a number of advanced numerical models are documented in the literature for more realistic prediction of nonlinear soil-foundation interaction effects from the research domain to a form useful for practical application. On the other hand, the characterization of seismic motions with respect to the exceedance of the design limits is conducted on the basis of displacement demands DD, following the logic of displacement-based design [9]-[12]. Accordingly, it is important to evaluate the nonlinear effects of SSI on seismic displacement demands of structures subjected to strong near-fault earthquakes. Furthermore, "coherent velocity pulses" hidden in near-fault ground motion records are identified as the driving force of large rocking amplitudes based on recent findings [13], [14]. Hence, it would be a promising idea to assess the vulnerability of rocking soil-structure systems to pulse-like earthquakes that cause (i) maximum rocking, and (ii) maximum drift demands.

In this paper, seismic vulnerability of uplift-permitted rocking structures to near-fault earthquakes is addressed. For this purpose, steel moment-resisting frame structures designed by current advanced codes of practice are investigated considering nonlinear SSI effects. 10-, 15-, and 20-story planar building frames with aspect ratio of 3 are considered with and without structural ductility, in order to investigate the coupling between superstructure and soil-foundation nonlinearities. Inelastic seismic demands of the superstructure are considered using concentrated plasticity model. The raft foundation system is designed for different soil types. Winkler model is used to represent the underlying soil. The substructure is assumed to be in three comparative condition (i) fixed base, (ii) linear SSI, and (iii) nonlinear SSI. To assess

F. M. Tehranizadeh is a professor in Amirkabir University of Technology, Tehran, Iran (phone: 009821-64543030; e-mail: dtehz@yahoo.com).

S. E. Shoushtari Rezvani is a Ms. graduate Student from Amirkabir University of Technology, Tehran, Iran (e-mail: sh.elmira88@gmail.com).

the effects of ground motion intensity, the suite of near-fault records used in this study is scaled to Design Basis Earthquake (DBE) as well as Maximum Credible Earthquake (MCE) levels.

II. Structural Design

In this paper, three steel frames of 10, 15, and 20 stories are studied. These frames are selected from three-dimensional structural modeling in which, to avoid the effects of geometrical asymmetry, plans are considered symmetric and similar. Each frame constitutes of three identical spans, and story height in all of them is 3 m. Since aspect ratio of the superstructure is assumed to be constantly equal to 3, the width of spans is 3.33, 5.0, and 6.67 m for the 10-, 15-, and 20-story buildings, respectively. Lateral seismic resisting system is special steel moment-resisting frame. For loading of structures, ASCE7-10 [15] is considered and the design dead and live loads are 550 and 200 kg/m^2, respectively. These gravity loads are distributed over the floor using a chessboard loading pattern. Structures are designed in fixed-base condition in accordance with the American Institute of Steel Construction AISC-05 [16]. Linear static and linear spectrum methods are used for designing the frames.

Steel profiles are all A36 with yielding strength of 2500 kg/cm2, ultimate strength of 4070 kg/cm^2 and elasticity module of 2 100 000 kg/cm^2. Its Poisson's ratio is 0.3 and its density is equal to 7833 kg/cm^3. Loading assumptions required in the ASCE7-10 are as follows: Seismic zone is assumed to be zone 4, which includes the near-fault effects. Soil type is considered stiff soil (SD) (as per the code's instructions, we can assume the soil type to be SD when no information is available). Occupancy factor (I=IP) is considered 1. Moreover, 0.2 and 1 s spectral response accelerations (S_s and S_1) are considered 1.5 and 0.6, respectively. Thus, values of site coefficients (F_a and F_v) will be 1 and 1.5. Table I shows the section properties of the designed members of the analysis model structures. To have a complete symmetric plan, all sections must have two axes of symmetry.

III. Analysis Methodology

Once the frame sections are designed assuming fixed-base superstructure, it is aimed to assess seismic performance of the soil-foundation-structure system in this study. Openly available software platform OpenSees [17] has been used for static and dynamic analyses. For nonlinear analysis, steel behavior is assumed bilinear, with secondary stiffness equal to 3%. Also, Rayleigh damping model was used, in which the damping ratio was assumed to be 5% of the critical damping for the first and fourth modes. Parameters that are chosen as performance indices of structure-foundation system in this paper include interstory drift demand, roof displacement, and maximum foundation tilting. First-mode natural period of frames are 0.89, 1.89 and 3.64 s for 10-, 15-, and 20-story structures, in the same order. Before studying the dynamic response of structures, it is helpful to check the structural capacity of each frame. For this purpose, an appropriate pattern (i.e. fundamental mode shape of fixed-base superstructure) for loading on height is used and frames are analyzed by nonlinear static analysis (pushover). Fig. 1 shows the capacity curves of the designed frames. This figure demonstrates that the 10-story structure has more normalized strength in comparison with other structures and its behavior pattern is close to bilinear. Indeed, due to the smaller natural period of 10-story structure, this structure has a larger base shear coefficient.

TABLE I
SECTION PROPERTIES OF THE DESIGNED STEEL FRAME MEMBERS

Story	Column			Beam
	A (cm^2)	$I_x = I_y$ (cm^4)	$r_x = r_y$ (cm)	I (cm^4)
10-Story Frame				
1-4	171	23210	11.7	21560
5-7	119	11190	9.7	21560
8-10	76	4585	7.8	21560
15-Story Frame				
1-5	385	117500	17.5	54530
6-10	304	73370	15.5	40370
11-15	171	23210	11.7	24390
20-Story Frame				
1-5	575	262200	21.4	79500
6-10	475	179100	19.4	79500
11-15	304	73370	15.5	54530
16-20	233	43010	13.6	26670

TABLE II
GEOTECHNICAL PROPERTIES OF SOIL

Soil Type	B	C	D
Density ρ (t/m3)	21	20	19
Shear modulus, G (MPa)	130	100	75
Poisson's ratio ϑ	0.35	0.35	0.35
Cohesion, C (kPa)	10	10	10
Friction angle $\emptyset$ (deg)	40	37	33
Shear wave velocity, Vs (m/s)	800	500	300

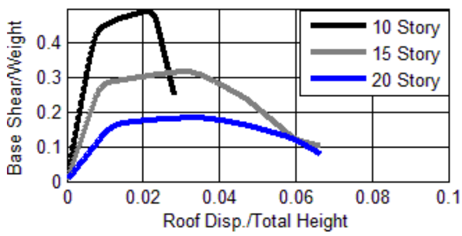

Fig. 1 Capacity curves of the designed steel frames using pushover analysis

IV. Soil-Foundation Modeling

The beam-on-nonlinear-Winkler foundation (BNWF) model is used in this study to simulate nonlinear soil-foundation interaction as schematically illustrated in Fig. 2. This model was proposed by Gajan et al. [18] and earlier by Harden and Hutchinson [19] and Harden et al. [20]. The BNWF model is also integrated with the openly available software platform OpenSees [17] by Raychowdhury and Hutchinson [21]. BNWF model with nonlinear springs of variable stiffness intensity can characterize the nonlinear, time dependent behavior of the foundation-soil interface for shallow foundations (footings, mats). Fig. 2 illustrates the 10-story steel frame of aspect ratio (H/B) equal to 3. The frame is supported by a surface raft foundation of length L_f.

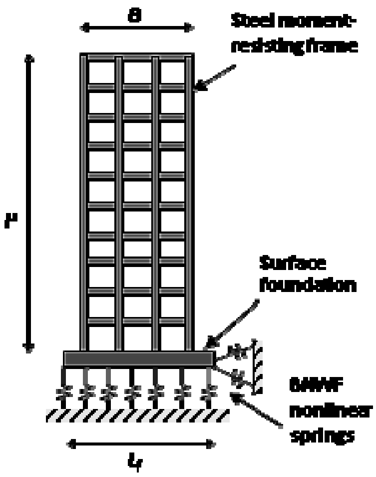

Fig. 2 Schematic diagram of soil-foundation-structure system using BNWF model

The BNWF model integrated with OpenSees, namely "ShallowFoundationGen" module, consists of elastic beam-column elements that capture the structural foundation behavior as well as independent zero-length soil elements to model the soil-foundation interaction. The parameters required for the BNWF model are related to soil and footing properties in addition to finite element mesh properties. In the OpenSees implementation, these parameters are divided into two broad categories: (i) user-defined parameters and (ii) hard-coded parameters.

Parameters of particular interest describing geotechnical properties of the subsoil are presented in Table II. These parameters are given for three soil types B, C, and D according to site classification introduced in ASCE7-10.

The next set of parameters describing structural properties of the foundation are presented in Table III. The design of the raft foundations have been done with respect to load bearing capacity of the underlying soil as well as settlement criteria based on recommendations of FEMA P-751 [22]. Vertical static safety factor of foundation (FS_v) is a key parameter controlling potential of foundation uplifting and soil plasticity during foundation-soil interactions. Low values of FS_v means statically heavily-loaded foundations that can exhibit significant level of nonlinearities during seismic loading.

Three comparative SSI conditions are considered in this study: first, "fixed-base" condition that means the foundation system and supporting soil are rigid; second, "linear SSI" condition, that means flexible foundation and soil but not allowed to uplift and no soil yielding; third, "nonlinear SSI" condition in which foundation uplifting and soil plasticity are included.

V. Ground Motion Records

The near-fault record set includes twenty-eight records (56 individual components) selected from the PEER NGA database as recommended by FEMA-P695 [23] for nonlinear dynamic analyses. Fourteen records have pulses (Pulse-like subset) and fourteen records do not have pulses (No-Pulse subset), as judged by wavelet analysis classification of the records [24].

TABLE III
Design Parameters of Raft Foundations With No Embedment

No. Story	Soil Type	L_f (m)	T_f (m)	FS_v
10	B	11	1.2	3.86
	C	11	1.2	2.30
	D	12	1.2	1.70
15	B	16	1.5	2.81
	C	17	1.5	2.04
	D	21	1.5	1.59
20	B	21	1.8	2.79
	C	27	1.8	2.14
	D	33	1.8	1.64

Table IV summarizes the magnitude as well as site and source characteristics of the selected ground motions. The ground motion set is recorded at sites less than 10 km from fault rupture. Event magnitudes range from M6.5 to M7.9 with an average magnitude of M7.0. Site characteristics including shear wave velocity and the corresponding NEHRP Site Class are presented in Table IV. Of the entire twenty-eight records, eleven sites are classified as Site Class D (stiff soil sites), fifteen are classified as Site Class C (very stiff soil sites), and the remaining two are classified as Site Class B (rock sites). Fourteen records are from events of predominantly strike-slip faulting and the remaining fourteen records are from events of predominantly thrust (or reverse) faulting.

To assess the effects of ground motion intensity, the suite of near-fault records used in this study is scaled to DBE and MCE levels based on scaling method provided by ASCE7-10 [15]. Fig. 3 depicts 5% damping elastic acceleration response spectra of the selected ensemble of 28 records after scaling, along with the design spectrum of the 15-story frame. As shown, the scaled records cover a wide range of seismic excitations, ranging from medium to strong intensity for different period intervals.

VI. Effects of Soil-Structure Interaction on Drift Demands

The statistical results of the structural analyses for the pulse-like and no-pulse ground motion sets are shown in Figs. 4 and 5 at DBE and MCE excitation levels, respectively. Mean value and maximum standard deviation (σ_{max}) of the maximum interstory drift demands (MIDD) for all stories are shown for each structure. Observe that the mean structural response is consistently higher for the pulse-like subset (left-hand columns of Figs. 4 and 5), even though the pulse-like and no-pulse ground motion have the same PGV. The predominant pulse hidden in pulse-like records leads to larger nonlinearities in the system and larger ductility demands. Moreover, since the structural response appears to be controlled by the predominant pulse, and this pulse varies widely from one ground motion to another, the dispersion in the structural response is larger for the pulse-like subset, as evidenced by the larger values of the maximum standard deviation (σ_{max}) drift demands when the rocking system is subject to pulse-like ground motions (left-hand columns of Figs. 4 and 5) as opposed to no-pulse records (right-hand columns of Figs. 4 and 5).

Comparing the results of Fig. 4 with those of Fig. 5 also confirms that reduction in drift demands due to nonlinear SSI with respect to linear SSI and fixed-base cases are amplified when the ground motion intensifies. Moreover, the reduction in drift demands due to nonlinear SSI is characterized by a more uniform distribution pattern along the height with less sensitivity to input excitation (i.e. less values of σ) when compared to the fixed-base and linear SSI condition.

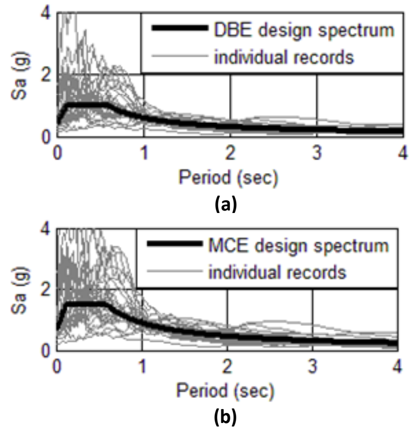

Fig. 3 Elastic response spectra of the selected ensemble of 28 records after scaling to a) DBE and b) MCE levels, along with the corresponding design spectra of the 15-story frame

TABLE IV
LIST OF NEAR-FAULT EARTHQUAKE RECORDS USED IN THIS STUDY [23]

ID No	Event			Station	Site Data		Source (Fault Type)
	Mw	Year	Name		Site Class	Vs_30 (m/s)	
			Pulse-like Records Subset				
1	6.5	1979	Imperial Valley-06	El Centro Array #6	D	203	Strike-slip
2	6.5	1979	Imperial Valley-06	El Centro Array #6	D	211	Strike-slip
3	6.9	1980	Irpinia, Italy-01	Sturno	B	1000	Normal
4	6.5	1987	Superstition Hills-02	Parachute Test Site	D	349	Strike-slip
5	6.9	1989	Loma Prieta	Saratoga - Aloha	C	371	Strike-slip
6	6.7	1992	Erzincan, Turkey	Erzincan	D	275	Strike-slip
7	7	1992	Cape Mendocino	Petrolia	C	713	Thrust
8	7.3	1992	Landers	Lucerne	C	685	Strike-slip
9	6.7	1994	Northridge-01	Rinaldi	D	282	Thrust
10	6.7	1994	Northridge-01	Sylmar - Olive View	C	441	Thrust
11	7.5	1999	Kocaeli, Turkey	Izmit	B	811	Strike-slip
12	7.6	1999	Chi-Chi, Taiwan	TCU065	D	306	Thrust
13	7.6	1999	Chi-Chi, Taiwan	TCU102	C	714	Thrust
14	7.1	1999	Duzce, Turkey	Duzce	D	276	Strike-slip
			No-Pulse Records Subset				
15	6.8	1979	Gazli, USSR	Karakyr	C	660	Thrust
16	6.5	1979	Imperial Valley-06	Bonds Corner	D	223	Strike-slip
17	6.5	1979	Imperial Valley-06	Chihuahua	D	275	Strike-slip
18	6.8	1985	Nahanni, Canada	Site 1	C	660	Thrust
19	6.8	1985	Nahanni, Canada	Site 2	C	660	Thrust
20	6.9	1989	Loma Prieta	BRAN	C	376	Strike-slip
21	6.9	1989	Loma Prieta	Corralitos	C	462	Strike-slip
22	7	1992	Cape Mendocino	Cape Mendocino	C	514	Thrust
23	6.7	1994	Northridge-01	LA - Sepulveda VA	C	380	Thrust
24	6.7	1994	Northridge-01	Northridge - Saticoy	D	281	Thrust
25	7.5	1999	Kocaeli, Turkey	Yarimca	D	297	Strike-slip
26	7.6	1999	Chi-Chi, Taiwan	TCU067	C	434	Thrust
27	7.6	1999	Chi-Chi, Taiwan	TCU084	C	553	Thrust
28	7.9	2002	Denali, Alaska	TAPS Pump Sta. #10	C	553	Strike-slip

This observation can be attributed to the rigid-body rotation of the rocking structure at the base level. It is also concluded that nonlinear SSI to some extent protects the superstructure from destructive effects of strong pulse-like ground motions.

Statistical results of Fig. 6 depict the SSI effects on drift demands when the ductility of the superstructure is neglected in seismic analyses, namely nonductile superstructure. The results confirm that ignoring the structural nonlinearities in seismic analyses does not significantly affect the rocking performance of the soil-foundation subjected to strong earthquakes. So that the overall patterns of drift demand distribution along height, as well as reduction magnitudes are rather similar when compared to the results of Fig. 5 for the corresponding ductile superstructure.

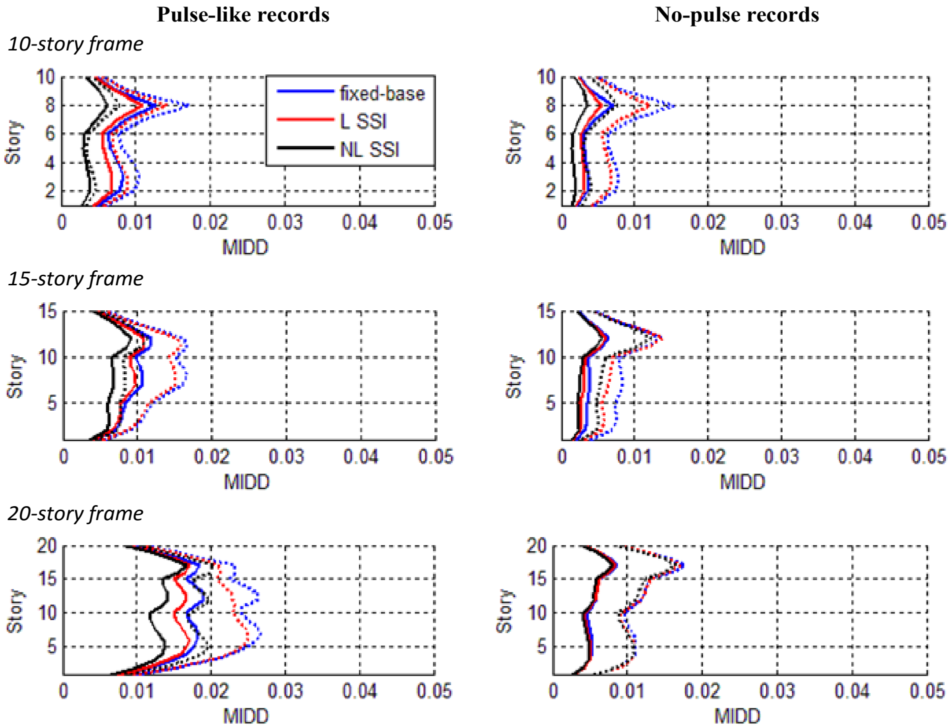

Fig. 4 Statistical results of MIDD distribution at “DBE” level (Dash lines indicate mean+□)

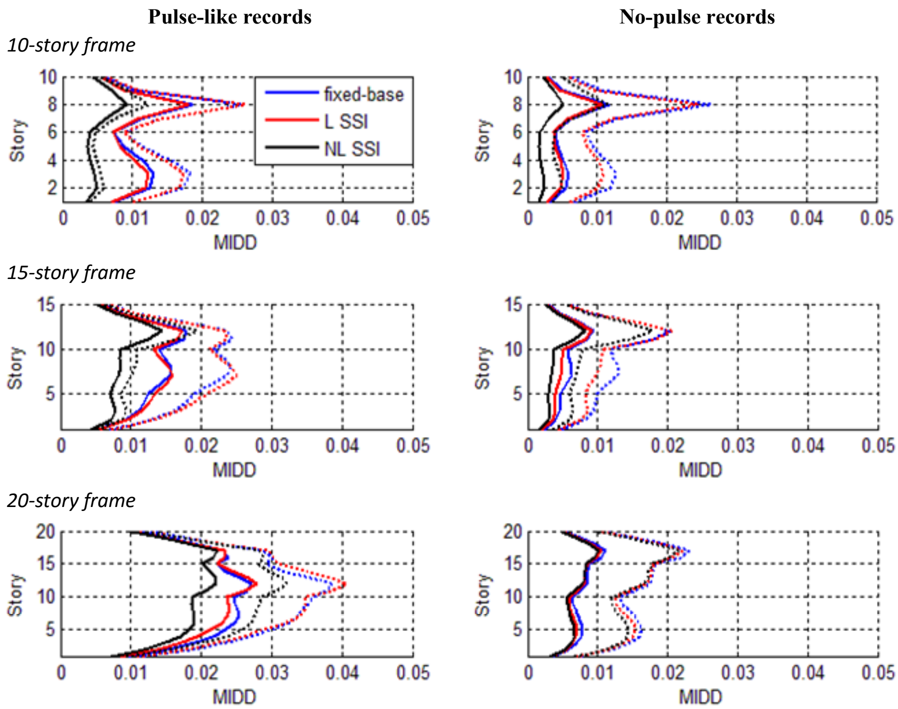

Fig. 5 Statistical results of MIDD distribution at “MCE” level (Dash lines indicate mean+σ)

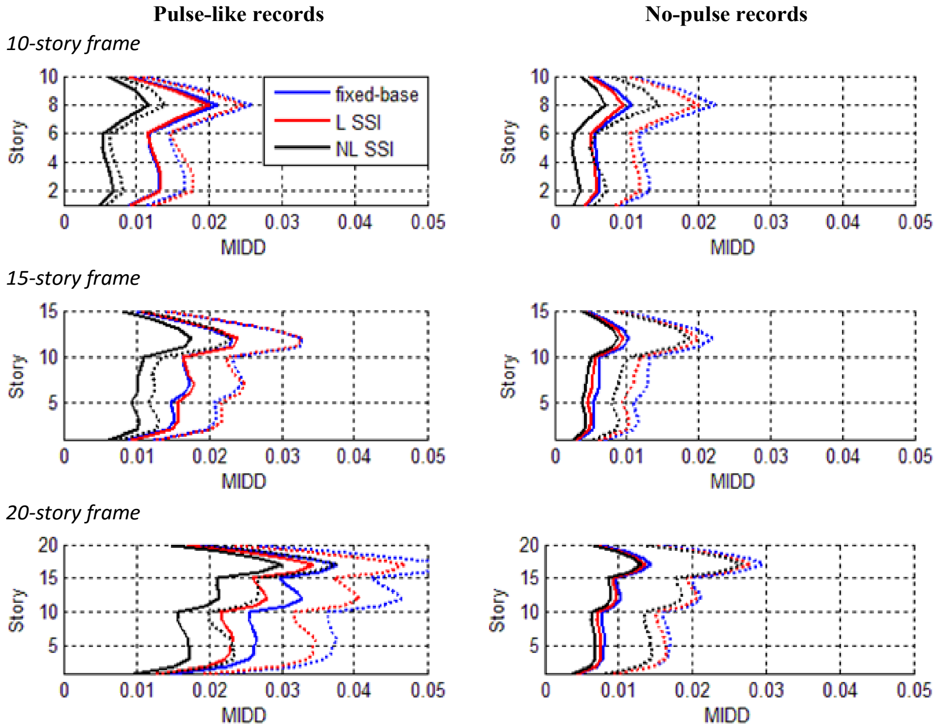

Fig. 6 MIDD distribution of “non-ductile” frame at MCE level (Dash lines indicate mean+σ)

VII. Rocking Response of Uplifted Foundation

The foundation rocking response of 10-, 15-, and 20-story structures subjected to pulse-like and no-pulse records are presented in Table V in terms of maximum absolute foundation tilting θ_f. This quantity can well represent the level of foundation rocking performance and consequently uplifting and soil plasticity incorporation. Evidently, θ_f values induced by pulse-like ground motions are significantly higher than those under no-pulse records with the same PGV. It is worth noting that the peak value of foundation tilting is mostly occurred at the beginning of the record due to arrival of the predominant pulse. This pulse imposes severe demands to the structure and the entire rocking soil-structure system. The arrival of the velocity pulse causes the rocking foundation to dissipate considerable input energy in relatively few plastic cycles. Furthermore, the mean values of maximum foundation tilting in case of elastic superstructure are almost twice those of its ductile counterpart at DBE excitation level. However, these values are almost the same when the excitation is scaled up to MCE level, except for mean rocking amplitude of the 20-story building. The dominant effect of pulses can be generalized and evaluated by comparing different rocking response of pulse-like records with that of no-pulse records at different intensity levels.

VIII. Conclusions

Seismic vulnerability of flexible rocking structures to near-fault earthquakes is investigated. For this purpose, steel moment-resisting frame structures designed by current codes of practice are focused considering nonlinear SSI effects. 10-, 15-, and 20-story planar building frames with aspect ratio of 3 are considered with and without structural ductility, in order to investigate the coupling between superstructure and soil-foundation nonlinearities.

TABLE V
Statistical Results of Foundation Rocking Performance in Terms of Max. Foundation Tilting

No. story	Type of record	Ductile superstructure		Nonductile superstructure	
		θ_{mean} (rad.)	σ	θ_{mean} (rad.)	σ
DBE level					
10	pulse-like	0.011	0.009	0.024	0.017
	no-pulse	0.005	0.003	0.011	0.006
15	pulse-like	0.009	0.008	0.019	0.015
	no-pulse	0.002	0.001	0.005	0.002
20	pulse-like	0.007	0.006	0.014	0.013
	no-pulse	0.003	0.003	0.006	0.008
MCE level					
10	pulse-like	0.024	0.016	0.024	0.017
	no-pulse	0.013	0.006	0.011	0.006
15	pulse-like	0.019	0.015	0.019	0.015
	no-pulse	0.005	0.002	0.005	0.002
20	pulse-like	0.008	0.005	0.014	0.013
	no-pulse	0.004	0.002	0.006	0.008

Inelastic seismic demands of the superstructure are considered using concentrated plasticity model. The raft foundation system is designed for different soil types. BNWF model is used to represent dynamic impedance of the underlying soil. The substructure is assumed to be in three comparative condition (i) fixed base, (ii) linear SSI, and (iii) nonlinear SSI. To assess the effects of ground motion intensity, the suite of near-fault records is scaled to DBE and MCE levels.

The results show that reduction in drift demands due to nonlinear SSI with respect to linear SSI and fixed-base cases are amplified when the ground motion intensifies (i.e. MCE level). Moreover, the reduction in drift demands due to nonlinear SSI is characterized by a more uniform distribution pattern along the height with less sensitivity to input excitation (i.e. less values of σ) when compared to the fixed-base and linear SSI condition. This observation can be attributed to the rigid-body rotation of the rocking structure at the base level. It is also concluded that nonlinear SSI considerably protects the superstructure from destructive effects of strong pulse-like ground motions.

According to the obtained results, it is obvious that neglecting the effects of nonlinear SSI can significantly bias the estimations of seismic structural demands especially under pulse-like ground motions. In order to more realistically evaluate the seismic performance of rocking structures supported by shallow foundation in the near-fault region, it is recommended to incorporate nonlinear SSI effects and conduct a site study to determine a design ground motion record or spectrum for the specific site soil conditions.

References

[1] Somerville P, Smith N, Graves R, Abrahamson N. “Modification of empirical strong ground motion attenuation relations to include the amplitude and duration effects of rupture directivity”. Seismological Society Letters 68(1): 180–203, 1997.

[2] Somerville P. “Development of an improved ground motion representation for near-fault ground motions”. SMIP98 Seminar on Utilization of Strong-Motion Data, Oakland, CA, 1998.

[3] Bolt BA. Earthquakes. W.H. Freeman: New York, NY, 1993.

[4] MacRae GA, Mattheis J. “Three-dimensional steel building response to near-fault motions”. Journal of Structural Engineering 126(1): 117–126, 2000.

[5] Chopra A, Chintanapakdee C. “Comparing response of SDF systems to near-fault and far-fault earthquake motions in the context of spectral regions”. Earthquake Engineering and Structural Dynamics 30(12): 1769–1789, 2001.

[6] Longjun X, Rodriguez-Marek A, Lili X. “Design spectra including effect of rupture directivity in near-fault region”. Earthquake Engineering and Engineering Vibration 5(2): 159–170, 2006.

[7] Applied Technology Council (ATC), “Tentative Provisions for the Development of Seismic Regulations for Buildings”, Report No. ATC 3-06, Redwood City, CA, 1978.

[8] FEMA, NEHRP Recommended Provisions for Seismic Regulations for New Buildings and Other Structures, Part 1: Provisions, FEMA 450-1/2003 Edition, prepared by the Building Seismic Safety Council for the Federal Emergency Management Agency, Washington, D.C, 2004.

[9] Bertero V State of the art report on: design criteria. In: Proceedings of 11th world conference on earthquake engineering, Acapulco, Mexico, Oxford, Pergamon, 1996.

[10] “Tassios TP Seismic design: state of practice”. In: Proceedings of 11th european conference on earthquake engineering, Rotterdam, AA Balkema, pp 255–267, 1998.

[11] “Priestley MJN Performance based seismic design”. In: Proc. 12th world conference on earthquake engineering (12WCEE), Auckland, New Zealand, Paper No. 2831, 2000.

[12] Faccioli E, Paolucci R, Vivero G “Investigation of seismic soil-footing interaction by large scale cyclic tests and analytical models”. In: Proc., 4th int. conf. recent advances in geotechnical earthquake engineering and soil dynamics, 2001.

[13] Acikgoz, S and DeJong, M.J “The interaction of elasticity and rocking in flexible structures allowed to uplift”. Earthquake Engineering and Structural Dynamics (published online: doi: 10.1002/eqe.2181), 2012.

[14] Acikgoz, S and DeJong, M.J, “Characterizing the Vulnerability of Flexible Rocking Structures to Strong Ground Motions”. Proc., 15WCEE, Lisbon, Portugal, 2012.

[15] ASCE-7. “Seismic Evaluation and Retrofit of Concrete Buildings. Structural Engineering Institute (SEI) and American Society of Civil Engineers (ASCE)”, Reston, Virginia, 2010.

[16] AISC (American Institute of Steel Construction). “Specification for Structural Steel Buildings”. AISC: Chicago, IL, 2005.

[17] PEER, Open system for earthquake engineering simulation (OpenSees) –development platform by the Pacific Earthquake Engineering Research Center (PEER), http://opensees.berkeley.edu/,2008.

[18] Gajan, S., Raychowdhury, P., Hutchinson, T. C., Kutter, B. L., and Stewart., J. P. “Application and Validation of Practical Tools for Nonlinear Soil-Foundation Interaction Analysis”, Earthquake Spectra 26(1), 111–129, 2010.

[19] Harden, C. W., and Hutchinson, T. C. “Beam-on-nonlinear-Winkler-foundation modeling of shallow”, rocking-dominated footings, Earthquake Spectra 25(2), 277–300, 2009.

[20] Harden, C. W., Hutchinson, T., Martin, G. R., and Kutter, B. L. “Numerical modeling of the nonlinear cyclic response of shallow foundations”, Report No.: PEER-2005/04, Pacific Earthquake Engineering Research Center, University of California, Berkeley, 2005.

[21] Raychowdhury, P., and Hutchinson, T. C. “Nonlinear material models for Winkler-based shallow foundation response evaluation,” Proc. of GeoCongress 2008: Characterization, Monitoring, and Modeling of GeoSystems, New Orleans, LA, ASCE Geotechnical Special Publication No. 179, A. N. Alshawabkeh, K. R. Reddy, and M. V. Khire (eds.), 686–693, 2008.

[22] “FEMA, NEHRP Recommended Seismic Provisions”: Design Examples, EMA P-751/2012, prepared by the Building Seismic Safety Council for the Federal Emergency Management Agency, Washington, D.C, 2009.

[23] Federal Emergency Management Agency (FEMA). “Quantification of building seismic performance factors”. FEMA P695, Washington DC, 2009.

[24] Baker, J. W. “Quantitative classification of near–fault ground motions using wavelet analysis,” Bulletin of Seismological Society of America 97(5), 1486–501, 2007.